

Unsteady Numerical Investigations of Flow and Heat Transfer Characteristics of Nanofluids in a Confined Jet Using Two-Phase Mixture Model

Mazaher Rahimi-Esbo*, Reza Mohammadyari, Seyed Majid Rahgoshay

Young Researchers and Elite Club, Buinzahar Branch, Islamic Azad University, Buinzahra, Iran

Received 12 April 2016;

revised 8 May 2017;

accepted 28 May 2017;

available online 1 January 2018

ABSTRACT: The development of high-performance thermal systems has increased interest in heat transfer enhancement techniques. The application of additives to heat transfer liquids is one of the noticeable effort to enhance heat transfer. In this paper two-dimensional unsteady incompressible nanofluid flow in a confined jet at the laminar flow regime is numerically investigated. The Mixture model is considered to simulate the nanofluid jet flow inside the channel. The governing mass, momentum equations for mixture and dispersed phase and energy equation for mixture are solved using the finite volume method. The result showed the relative velocity is very small and negligible and the nanoparticles concentration distribution is uniform. Results have been reported at different Reynolds numbers for steady asymmetric jet development at various values of the duct-to-jet width ratio (aspect ratio) and different volume fractions of nanoparticles. The present computations are in a very good agreement with experimental and numerical results in open literature.

KEYWORDS: Aspect ratio; Mixture model; Nanofluids; Nusselt number; Recirculation region

INTRODUCTION

Convective heat transfer can be enhanced passively by changing flow geometry, boundary conditions, or by enhancing thermal conductivity of the fluid. Various techniques have been proposed to enhance the heat transfer properties of fluids. Researchers have also tried to increase the thermal conductivity of base fluids by suspending micro- or larger-sized solid particles in fluids, since the thermal conductivity of solid is typically higher than that of liquids. However, due to the large size and high density of the particles, there is no good way to prevent the solid particles from settling out of suspension. The lack of stability of such suspensions induces additional flow resistance and possible erosion. Modern nanotechnology provides new opportunities to process and produce materials with average crystallite sizes below 50 nm. Fluids with suspended nanoparticles are called nanofluid, a term proposed in 1995 by Choi [1] of the Argonne National Laboratory, U S A. Nanofluids can be considered to be the next generation heat transfer fluids because they offer exciting new possibilities to enhance heat transfer performance compared to pure liquids. They are expected to have superior properties compared to conventional heat transfer fluids, as well as fluids containing micro-sized metallic particles. The much larger relative surface area of nanoparticles, compared to those of conventional particles, should not only significantly improve heat transfer capabilities, but also should increase the stability of the suspensions.

Also, nanofluid can improve abrasion-related properties as compared to the conventional solid/fluid mixtures. To explain the reasons for the anomalous increase of the thermal conductivity in nanofluid, Kebabian et al. [2] proposed four possible mechanisms, e.g., Brownian motion of the nanoparticles, molecular-level layering of the liquid at the liquid/particle interface, the nature of heat transport in the nanoparticles, and the effects of nanoparticles clustering. In this paper contemporaneous effect of adding copper nanoparticles and jet flow on improvement of heat transfer properties in a duct is investigated. Also the effect of aspect ratios (duct width / jet width) on flow features and heat transfer properties is investigated. Jet flows are encountered in a wide variety of applications, such as gas turbine combustors, industrial burners, ejector systems, rocket nozzles, etc. Jet impingement has been explored as a cooling option in microelectronics. Recently, interest has been expressed by the automotive industry in exploring jet impingement for cooling power electronics components. Some researchers such as Li et al. [3] presented some applications of confined single submerged jets. The variation of critical Reynolds number for bifurcation with aspect ratio has been investigated in details by Battaglia et al. [4]. They have also validated their numerical predictions by comparing with the experimental data of Durst et al. [5]. Some researchers applied homogenous and two phase nanofluid flow in different applications. Rahimi-Esbo et al. [6] numerically studied force convection of turbulent nanofluid flow in a headbox. Their results showed that by increasing the Reynolds number, aspect ratio and volume fraction the average Nusselt number will increase.

*Corresponding Author Email: mrahimi@nutt.ac.ir
Tel.: +989116277073; Note. This manuscript was submitted on April 12, 2016; approved on May 8, 2017; published online January 1, 2018

Nomenclature	
AR	aspect ratio ($= h/d$)
c	mass fraction
C_D	drag coefficient
C_p	specific heat (kJ/kg K)
d	jet length (m)
d_p	average diameter of nanoparticles (m)
h	height of channel (m)
i, j	indices
k	thermal conductivity (W/m K)
Nu	Nusselt number
P	pressure (Pa)
P_r	Prandtl number of nanofluid
Q	heat flux (W/m ²)
R_e	Reynolds number
T	temperature (K)
T_B	bulk temperature of nanofluid (K)
V	velocity (m/s)
Greek Symbols	
Φ_p	nanoparticle volume fraction (%)
Φ_{pm}	nanoparticle volume fraction for maximum packing
μ	density
μ^*	corrective viscosity coefficient
ρ	density (kg/m ³)
Subscripts	
avg	average
c	continuous phase
f	base fluid
in	Inlet
m	mixture
nf	nanofluid
p	particle

In their research the nanoparticles and the base fluid (i.e. water) were assumed to be in thermal equilibrium and no slip condition occurs between them. Also Rahimi-Esbo et al. [7] studied forced convection of turbulent jet flow in a converging sinusoidal channel and reported the same results. Heris et al. [8] investigated laminar flow forced convection heat transfer of Al₂O₃/water inside a circular tube with constant wall temperature experimentally. The Nusselt numbers of nanofluids were obtained for different nanoparticle concentrations as well as various Peclet and Reynolds numbers. Experimental results emphasize the enhancement of heat transfer due to the nanoparticles presence in the fluid. Heat transfer coefficient increases by increasing the concentration of nanoparticles in nanofluid. The increase in heat transfer coefficient due to presence of nanoparticles is much higher than the prediction of single phase heat transfer correlation used with nanofluid properties. Behzadmer et al. [9] studied numerically turbulent forced convection heat transfer in a circular tube with a nanofluid consisting of water and 1 vol. % Cu. Two phase mixture model has been implemented for the first time to study such a flow field. A single phase model formulation, which has been used frequently in the past for heat transfer with nanofluids, is also used for comparison with the mixture model. Their comparison of calculated results with experimental values shows that the mixture model is more precise than the single phase model. The axial evolution of the flow field and fully developed velocity profiles at different Reynolds numbers are also presented and discussed. Hwang et al. [10] measured the pressure drop and convective heat transfer coefficient of water-based Al₂O₃ flowing through a uniformly heated circular tube in the fully developed laminar flow regime. Experimental results show that the convective heat transfer coefficient enhancement exceeds, by a large margin, the thermal conductivity enhancement. They propose that flattening of velocity profile is a possible mechanism for the convective heat transfer coefficient enhancement

exceeding the thermal conductivity enhancement. Al-Aswadi et al. [11] investigated laminar forced convection flow of different nanofluids over a 2D horizontal backward facing step placed in a duct. They reported that the reattachment point moves downstream far from the step as Reynolds number increases, and nanofluid containing SiO₂ nanoparticles has the highest velocity among the other nanofluid types, while nanofluid of Au nanoparticles has the lowest velocity. Santra et al. [12] simulated copper-water nanofluid flow in an isothermally two-dimensional rectangular duct. They investigated the effect of Newtonian as well as non-Newtonian fluid for a wide range of Reynolds number and nanoparticles volume fraction. They reported heat transfer increases for increase in solid volume fraction for any Reynolds number. This increment was more or less same for both the Newtonian and non-Newtonian nanofluid, particularly for lower Reynolds number. Kalteh et al [13] numerically investigated laminar forced convection heat transfer of a copper-water nanofluid inside an isothermally heated microchannel. They used an Eulerian two-fluid model for simulating the nanofluid flow. They reported the two-phase modeling results show higher heat transfer enhancement in comparison to the homogeneous single-phase model. Alinia et al [14] numerically studied mixed convection of a nanofluid flow consisting of SiO₂ nanoparticles in an inclined enclosure cavity. They used two-phase mixture model to investigate the thermal behaviors of the nanofluid. Their results revealed that addition of nanoparticles enhances heat transfer in the cavity remarkably and causes significant changes in the flow pattern.

Although many researches are recorded in the field of nanofluid but in this paper for the first time two phase laminar nanofluid jet flow in a channel is numerically investigated. The aim of this study is to obtain an understanding of the velocity and temperature distribution, Nusselt number along both top and bottom walls downstream from the jet. Moreover, the performance of the

jet flow at various Reynolds number is investigated. Also the effect of nanoparticles on thermal and flow characteristics and the effect of aspect ratios on flow features and heat transfer properties are investigated. In this research copper nanoparticle which its thermal conductivity is approximately six hundred times bigger than water is used.

MODEL DESCRIPTION AND MATHEMATICAL FORMULATION

The unsteady two phase 2D laminar incompressible jet flow is considered. The mixture model is based on a single fluid two phase approach. Each phase has its own velocity and own volume fraction. For simplicity, the jet is taken isothermal. The velocity profile at the jet inlet is taken as parabolic one. The geometry considered and the flow configurations used are shown in Figure 1. Constant heat flux condition is taken for the top and bottom walls. The slip velocity between nanoparticles and flow is considered. The other boundary conditions are mentioned in Figure 1.

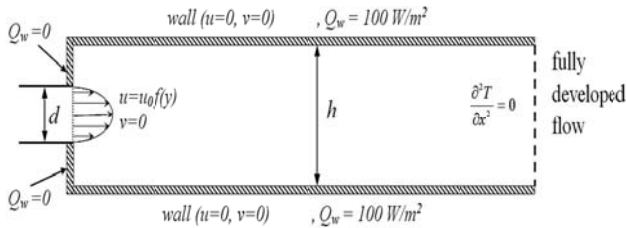


Fig. 1. Geometry and boundary condition of the problem

The thermo-physical properties of nanoparticles are given in Table 1.

Aspect ratio is taken as:

$$AR = h / d \quad (1)$$

The continuity and momentum equations are given by Maninen et al. [15] and following as:

Continuity equation for mixture:

$$\frac{\partial \rho_m}{\partial t} + \nabla \cdot (\rho_m V_m) = 0 \quad (2)$$

Where

$$V_m = \frac{1}{\rho_m} \sum_{k=1}^n \phi_k \rho_k u_k = \sum_{k=1}^n c_k u_k \quad (3)$$

Continuity equation for dispersed phase:

$$\frac{\partial \phi_p}{\partial t} + \nabla \cdot (\phi_p V_m) = -\nabla \cdot \left[\phi_p \phi_c \frac{\rho}{\rho_m} (V_p - V_c) \right] \quad (4)$$

Momentum equation for mixture:

$$\begin{aligned} \frac{\partial \rho_m V_m}{\partial t} + \nabla \cdot (\rho_m V_m V_m) &= -\nabla p + \nabla \cdot \tau_{Gs} + \rho_m g - \\ \nabla \cdot \left[\phi_p \rho_p \left(1 - \frac{\phi_p \rho_p}{\rho_m} \right) (V_p - V_c) (V_p - V_c) \right] & \quad (5) \\ \tau_{Gs} &= (\mu_m) \left[\nabla V_m + (\nabla V_m)^T \right] \end{aligned}$$

Momentum for dispersed phase (slip velocity equation):

$$\begin{aligned} |V_p - V_c| (V_p - V_c) &= \frac{4d_p}{3C_D} + \\ \left(\frac{\rho_p - \rho_m}{\rho} \right) \left[g - (V_m \cdot \nabla) V_m - \frac{\partial V_m}{\partial t} \right] & \quad (6) \end{aligned}$$

Where:

$$C_D = \begin{cases} 24(1 + 0.1 \text{Re}_p^{0.75}), & \text{Re}_p \leq 1000 \\ 0.45 \left(\frac{1 + 17.67f(\phi_p)}{18.87f(\phi_p)} \right)^{\frac{6}{7}}, & \text{Re}_p > 1000, \\ f(\phi_p) = \sqrt{1 - \phi_p} \left(\frac{\mu_c}{\mu_m} \right) \end{cases} \quad (7)$$

$$\begin{aligned} \text{Re}_p &= \left(\frac{dp \sqrt{u_{cp_0}^2 + v_{cp_0}^2} \rho_f}{\mu_m} \right), \\ \mu_m &= \mu_f \left(1 - \frac{\phi_p}{\phi_{pm}} \right)^{-2.5 \phi_{pm} \mu^*} \\ \mu^* &= \frac{\mu_p + 0.4 \mu_f}{\mu_p + \mu_f}, \phi_{pm} = 0.62 \end{aligned}$$

The energy equation for the 2D flow problem are given by Ishii et al. [16] and following as:

$$\begin{aligned} \frac{\partial (\rho_m C_{p_m} T)}{\partial t} + \nabla \cdot (\rho_m V_m C_{p_m} T) &= \nabla \cdot (K_{eff} \nabla T_m) - \\ \nabla \cdot \left(\phi_p \frac{\rho_f \rho_p}{\rho_m} V_{2j} T ((c_p)_f - (c_p)_p) \right) & \quad (8) \end{aligned}$$

Where V_{2j} is drift velocity and defined as following:

$$V_{2j} = -\phi_p (V_c - V_p) \quad (9)$$

The nondimensional flow and heat transfer parameters are defined as:

$$\text{Re} = 2\rho_f U_{in} d / \mu_f \quad (10)$$

$$Nu = 2hK_m \partial T / \partial y / (k_f(T_w - T_B)) \quad (11)$$

The Nusselt number is compared with the predictions of the well known Shah equation for laminar flows under the constant heat flux boundary condition:

$$Nu = 1.953 \left(\text{RePr} \frac{D}{x} \right)^{1/3} \quad \text{for} \quad \left(\text{RePr} \frac{D}{x} \right) \geq 33.3$$

$$Nu = 4.364 + 0.0722 \text{RePr} \frac{D}{x} \quad \text{for} \quad \left(\text{RePr} \frac{D}{x} \right) < 33.3 \quad (12)$$

THERMOPHYSICAL PROPERTIES OF NANO FLUID

Effective thermal conductivity:

The thermal conductivity of the nanofluid is calculated from the following equation:

$$K_m = ((1-\phi_p) \times (\rho K)_f + \phi_p \times (\rho \times K)_p) / \rho_m \quad (13)$$

Density and specific heat

The density and specific heat of the nanofluids are calculated by using the following correlations:

$$\rho_m = \sum_{k=1}^n \phi_k \rho_k$$

$$(Cp)_m = ((1-\phi_p) \times \rho_f \times (Cp)_f + \phi_p \times (\rho \times Cp)_p) / \rho_m \quad (14)$$

Effective Viscosity

In mixture model application the most often used correlation for the apparent viscosity of mixture is that according to Ishii and Zuber [16]. The general expression for the mixture viscosity is given by

$$\mu_m = \mu_f \left(1 - \frac{\phi_p}{\phi_{pm}} \right)^{-2.5 \phi_{pm} \mu^*} \quad (15)$$

Where $\phi_{pm}=0.62$ is the concentration for maximum packing and μ^* is the corrective viscosity coefficient that calculated by the following equation:

$$\mu^* = \frac{\mu_p + 0.4\mu_f}{\mu_p + \mu_f} \quad (16)$$

NUMERICAL PROCEDURE AND CODE VALIDATION

A finite volume technique on a collocated grid was implemented for discretizing the governing equations inside

the computational domain. The SIMPLE algorithm was used to link the pressure and velocity fields. For the stability of the solution, the diffusion term in the momentum equations is approximated by the second order central difference. Moreover, a deferred correction scheme is adopted for the convective terms. For discretizing the unsteady term implicit Euler method and tree times level scheme with time step of 0.1 is applied. An in-house code is applied using SIMPLE algorithm for forced convection jet flow in a channel. As depicted in Figure 2 the grid is highly concentrated close to the jet in order to ensure the accuracy of the numerical simulations and for saving both the grid size and the computational time.

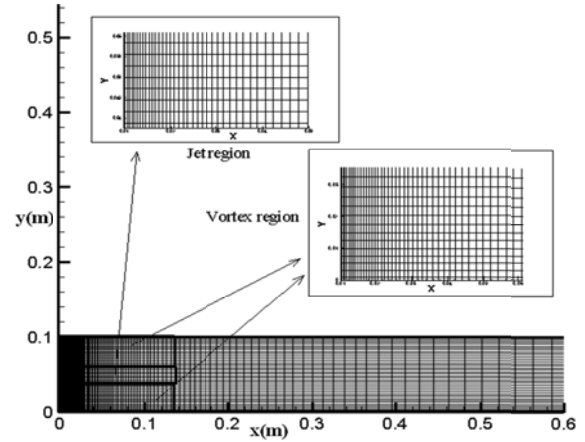


Fig. 2. Employed mesh geometry in the modeling

The convergence criterion required that the maximum sum of the error for each of the conserved variables be smaller than 1×10^{-5} . Grid densities of 10×200 , 20×400 , 40×800 and 80×1600 were selected to perform a grid independency test and they show less than 1% difference in Nusselt number compared to the chosen grid (40×800). This claim is shown in Figure 3.

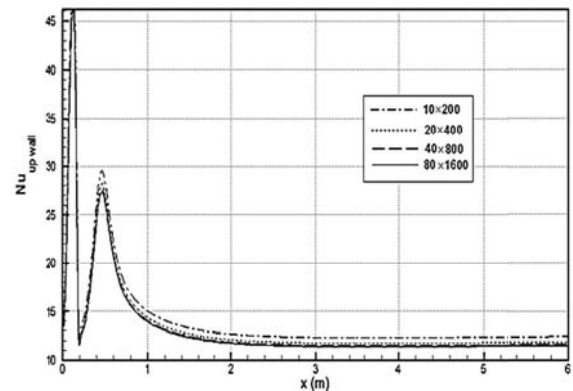


Fig. 3. Nusselt number on up wall at $\text{Re}=100$, $\text{AR}=16$ and $\Phi=0.02$

The results are compared with the simulation of Battaglia et al. [4] and experimental data of Durst et al. [5]. As it can be seen from Figure 4 there is a tolerable accuracy.

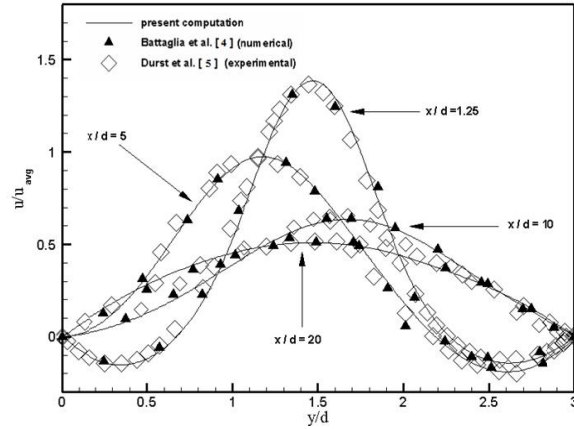


Fig. 4. Streamwise velocity profile at different axial position of the asymmetric jet at $Re = 80$ and $AR=3, \Phi = 0$

For the case of existence nanoparticles in a backward facing, the geometry and its boundary conditions are based on a study done by Al-Aswadi et al [11] for validation

purposes. The present results show a very good agreement with their results as shown in Figure 5.

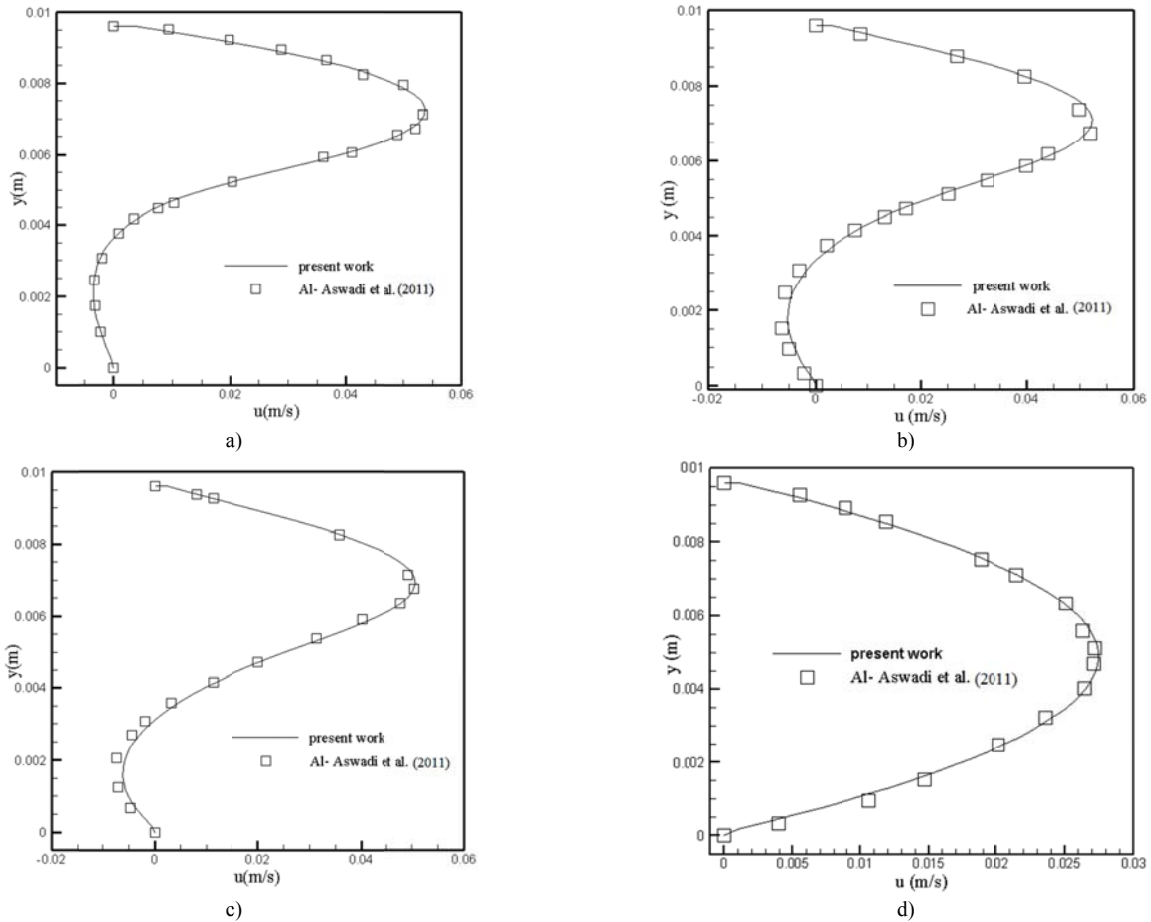


Fig. 5. Velocity distributions of SiO_2 nanofluid for a backward facing at $Re=175$ at different X/h ; (a) 1.04, (b) 1.92, (c) 2.6, (d) 32.8

The recirculation region is clearly appeared in Figure 5(a-b), where the recirculation region size decreases as the

flow transfer far downstream from the step. As the flow reaches the reattachment point the flow initiate to become

fully developed and it become more pronounced as the flow transfer farther along the wall downstream from the reattachment point as shown in Figures 5(c-d).

The two phase Mixture model results are compared with experimental results of Wen and Ding, [17], equation of Shah, numerical results of Lotfi et al. [18] and single phase model (Chon et al. [19] for thermal conductivity and Masoumi et al. [20] for viscosity of nanofluids) under the constant heat flux boundary condition in a tube. As it is obvious from the Figure 6 the Mixture model predicts the experimental results more accurately than the single-phase models and Shah equation.

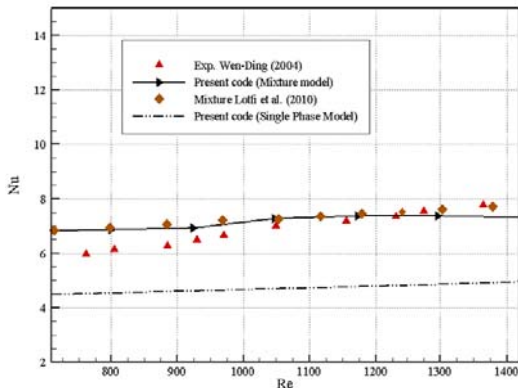


Fig. 6. Fully developed Nusselt number in a tube

It should be noted that Hwang [10] showed that convective heat transfer coefficient of nanofluids in laminar flow cannot be predicted by Shah equation. Furthermore For the validation of code at jet flow in a channel, in Figure 7 results are compared to experimental data of Lee at al. [21] for $Re = 120$, $H/B = 6$, and $B = 1.0$ mm, and the numerical prediction results from Chiriac and Ortega [22] for $Re = 125$ and $H/B = 5$, as well as numerical prediction results from Lee et al. [23] for $Re = 125$ and $H/B = 5$. H is the height of channel and B is the widths of jet.

RESULTS AND DISCUSSION

Simulations are performed for different Reynolds numbers of 25, 100, 200, 400, 600 and 800 and various volume fraction of nanofluid 2%, 4%, 6%, 8% and 10% are compared to their pure base fluid (water). Furthermore the simulations are carried out for different aspect ratios of 2, 4, 8, 16 and 32.

The flow expands from the fully developed parabolic profile from the jet and separates to form a primary recirculation region at upper and lower plate. It can be seen from the streamline contours that at a higher Reynolds number a third recirculation zone has developed downstream. The jet separates from the lower wall, impinges on the upper wall, and then reattaches to the lower wall. After that, the velocity profile reattaches and redevelops approaching a fully developed flow as fluid flows towards the channel exit.

Two phase mixture model results in a straight channel are compared with those of single phase model. Two different models for thermal conductivity [19,24] and viscosity [20,25] are applied.

As it can be seen from Figure 8 the two-phase modeling results show higher heat transfer enhancement in comparison to homogeneous single-phase model. It should be noted that models which consider the effect of temperature, Brownian motion, diameter of nanoparticles and etc showed a higher Nusselt than those of which only take volume fraction of nanoparticles for consideration in their equation.

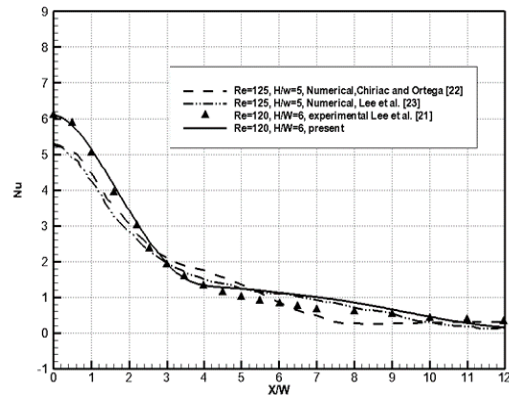


Fig. 7. Comparison of the lateral variation of local Nusselt number from different

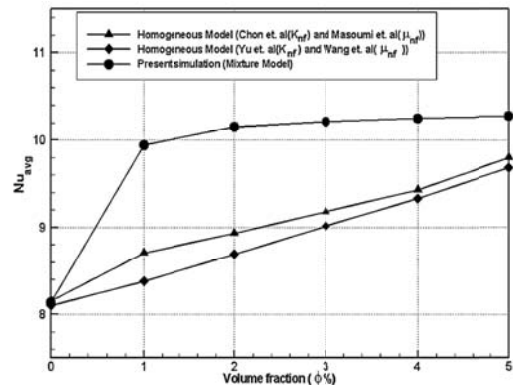


Fig. 8. Averaged Nusselt number at AR=1 and Re=100

Figure 9 shows the particle volume concentration and flow Reynolds number effect on the average Nusselt number. It can be seen that the average Nusselt number increases with an increase in the nanoparticles volume concentration as well as an increase in the flow Reynolds number. This behavior is expected since the higher nanoparticles concentration increases the thermal conductivity of the nanofluid and higher Reynolds number raises the length of the recirculation zones thus cause an increase in the heat transfer rate. Also, the Figure shows that the average Nusselt number is more sensitive to volume fraction than to Reynolds number.

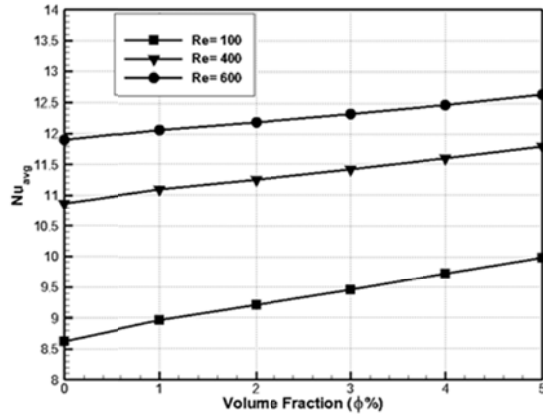


Fig. 9. Average Nusselt number on up wall at AR=4

In Figure 10 the effect of volume fraction on Nusselt number is presented. The effect of volume fraction of nanoparticles on the temperature gradient term and on the thermal conductivity ratio term is more pronounced. Nusselt number strongly increases for increasing particle concentration but temperature difference decrease on the wall is negligible. Before the point of reattachment, as the volume fraction percentage of nanoparticles increases the temperature gradient increases at the top wall.

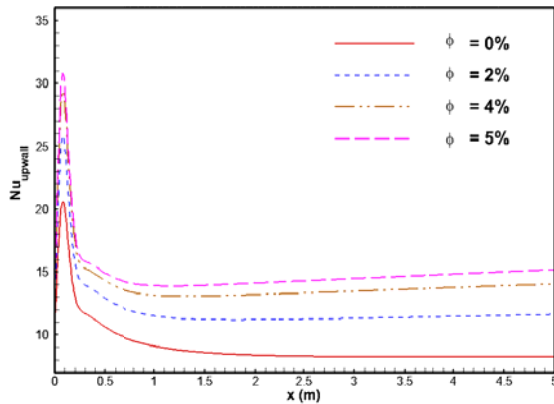


Fig. 10. Nusselt number on up wall at AR=4 and Re= 100

This is related to the addition inertia forces as depicted by equation 5.

The equations show that any increase in volume fraction increases inertia forces because ρ_m will be increased and accordingly increases the temperature gradient. Besides, the nanoparticles increase the thermal conductivity ratio term as it can be seen in equation 13. Therefore, both the temperature gradient term and thermal conductivity ratio term enhance by increasing the volume fraction of nanoparticles.

Accordingly, it can be seen that with increasing volume fraction the Nusselt number will be increased, because the heat transfer properties are improved. Two sudden growths are seen arrangement at the position of vortex zone. Down wall Nusselt number includes pre mention procedure.

At high Reynolds number and aspect ratio asymmetric flow was observed at jet flow in a channel in a steady solution. So an unsteady solution was seemed to be necessary. For the case of AR=16, Re=100 unsteady solution is applied and the streamline and temperature contour simultaneously is depicted in Figure 11. It is observed that after $t=7800$ seconds the streamline remain fixed.

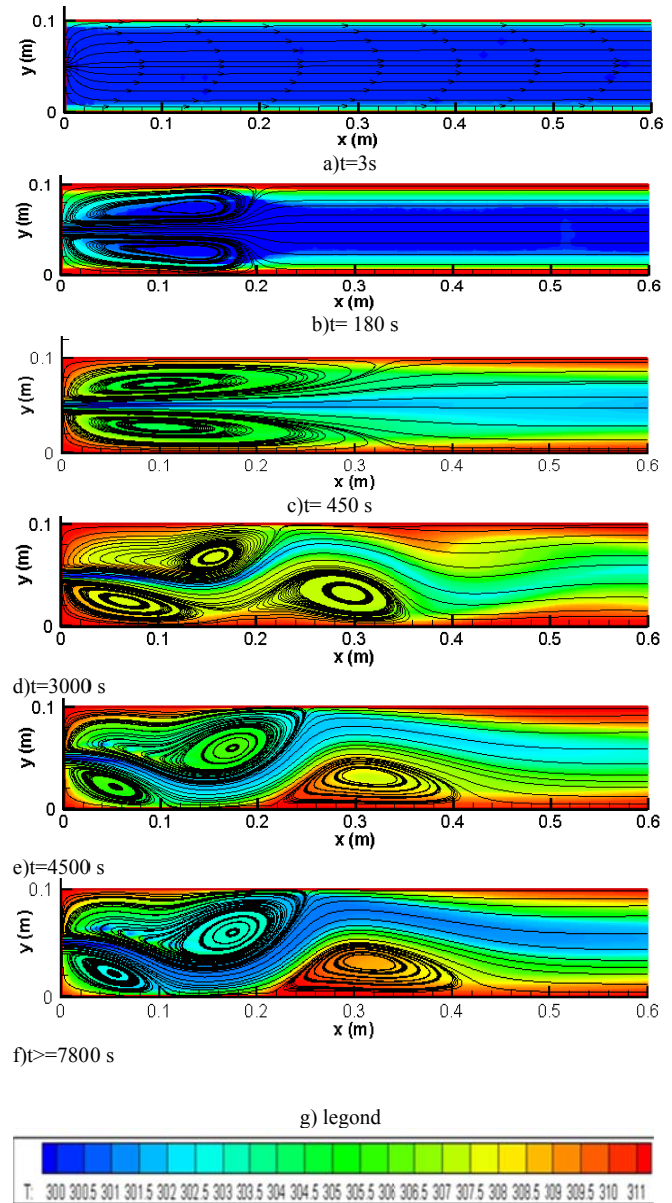


Fig. 11. Streamlines and temperature contours at Re=100 and AR=16

According to Figure 11 asymmetric flow occurs for both steady and unsteady cases. It should be noted that the asymmetry in the flow pattern corresponds to a bimodal steady configuration with the jet turning upwards or downwards in a random manner, during any computational run. Sarma et al. [26] presented this behavior in their

papers. According to the above proof the steady solution can be generalized to the unsteady problem. From now on results are reported on the steady state condition.

In **Error! Reference source not found.**Figure 12 the steady state streamline and temperature contour patterns at different aspect ratios is depicted.

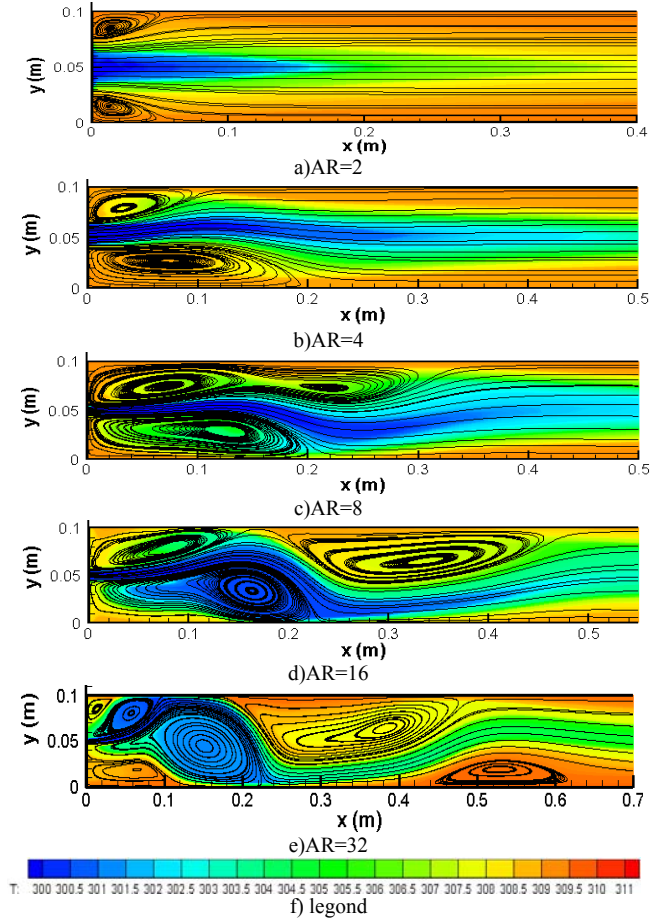


Fig. 12. Streamline and Temperature contours for different aspect ratio at $Re=100, \Phi=0\%$

It is observed that for a low aspect ratio such as $AR=2$, the jet develops almost symmetrically and back-flow are seen immediately after the sudden expansion. The jet decay is rapid and the transition from jet-to-duct flow occurs in a short distance.

At a higher aspect ratio of $AR=32$, it is observed that the steady state jet flow development is asymmetric and the transition from jet-to-duct flow occurs over a longer distance as well.

For describing unusual increasing of Nusselt number at high aspect ratios the streamlines contour and Nusselt number distributions are depicted in Figure 13. This unusual increasing is related to recirculation regions. When the separation occurred, because of chaotic of flow and

more contact to walls, this unusual increasing will be occurred.

As it can be seen the increasing is started with creation of vortexes and ended with stopping recirculation zones. So, the intensification of turbulence, suppression of the boundary layer, dispersion of the suspended particles, besides the augmentation of thermal conductivity and the heat capacity of the fluid were suggested to be the main reasons for heat transfer enhancement.

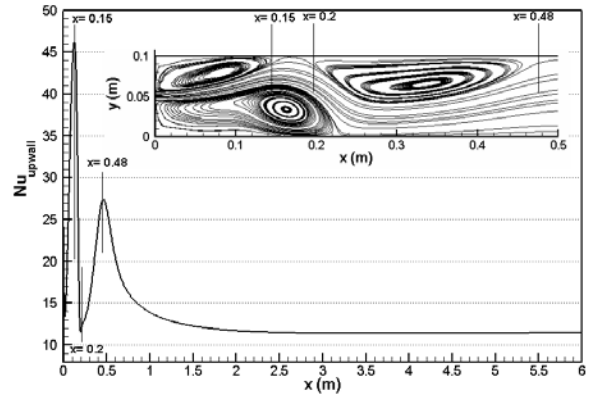


Fig. 13. Nusselt number and stream lines on up wall at $Re=100, AR=16$

In Figure 14 the steady state streamline patterns at different Reynolds numbers are depicted.

In this Figure the effect of Reynolds number on flow structure at $AR=4$ is shown. It is observed that for a low Reynolds number such as $Re=25$, the jet development is almost symmetric and counter-rotating velocities are seen immediately after the sudden expansion. The jet decay is rapid and the transition from jet-to-duct flow occurs in a short distance. At a higher Reynolds number of $Re=100$, it is observed that the steady state jet flow development is asymmetric.

Also, the transition from jet-to-duct flow occurs over a longer distance. For a still higher Reynolds number of 600, it is seen that asymmetric flow exhibits a wavy pattern with a larger wavelength and the flow development inside the duct occurs over a larger axial distance. It should be noted that the asymmetry in the flow pattern corresponds to a bimodal steady configuration with the jet turning upwards or downwards in a random manner, during any computational run.

In Figure 15 the x-direction velocity profile for different aspect ratios at $x=0.06m$ is depicted.

It is found that the velocity decreases as aspect ratios increase, because the length of recirculation region increases and the flow reattaches in a farther distance from the jet.

Furthermore, the peaks become sharper as aspect ratio increases due to the free hydrodynamic flow far from the walls friction and the friction between the opposite fluids flow directions. The recirculation region is clearly appeared in $AR=4, 8, 8$ and 32.

In Figure 16 the x-direction velocity profile at centerline of the duct for different aspect ratios is depicted. It is found that the velocity wave decreases as aspect ratios increases, the length of recirculation region increases and the flow reattaches in a farther distance from the jet. The penetration of jet in the channel enhances and jet decay is slow.

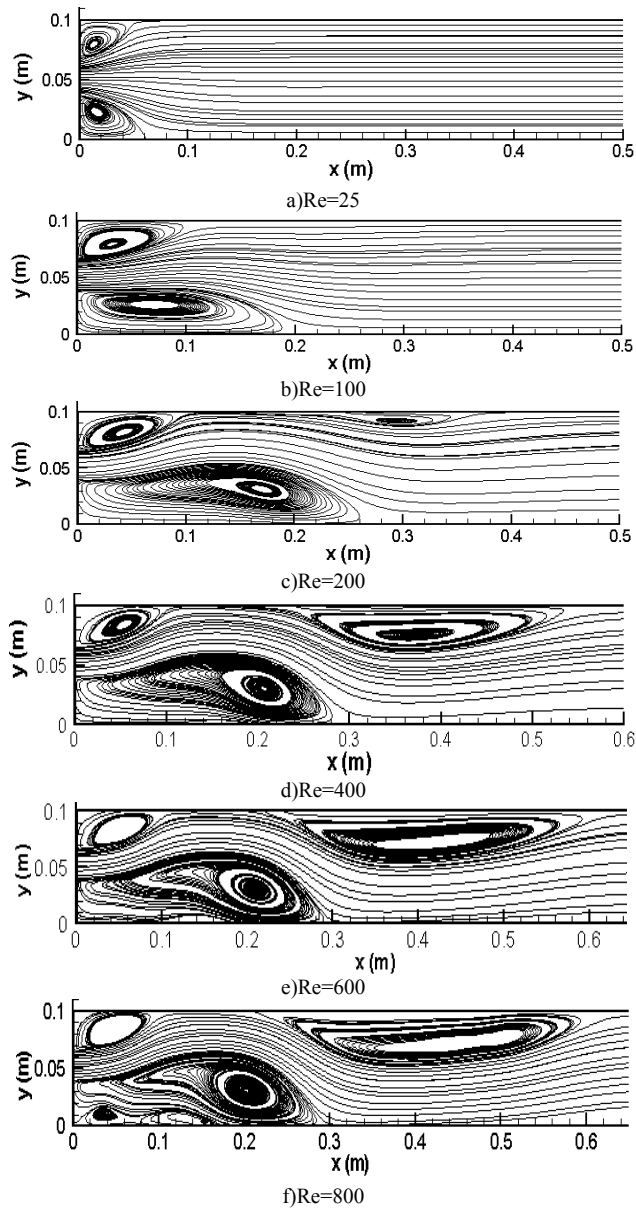


Fig. 14. Streamline contours for different Reynolds number at AR=4 and $\Phi=0\%$

CONCLUSION

For the first time two phase forced convection of nanofluid jet flow in a duct has been numerically studied. The Mixture model is applied for simulating. It has been observed that the relative velocity is very small and negligible and the nanoparticles concentration distribution is uniform. However, the two-phase modeling results show

higher heat transfer enhancement in comparison to the homogeneous single-phase model. The results show that by increasing the Reynolds number, aspect ratio and volume fraction the average Nusselt number will increase. By increasing aspect ratio from 2 to 32, as a result of the simultaneous increase in the developing length, penetration of the jet flow in to the duct, and length of the recirculation zones, more than 26 percent enhancement in averaged Nusselt number on the up wall is detected. These effects have 42 percent enhancement in averaged Nusselt number on down wall by increasing Reynolds number from 100 to 800.

It should be noted the intensification of turbulence, suppression of the boundary layer, dispersion of the suspended particles, besides the augmentation of thermal conductivity and the heat capacity of the fluid were suggested to be the possible reasons for heat transfer enhancement.

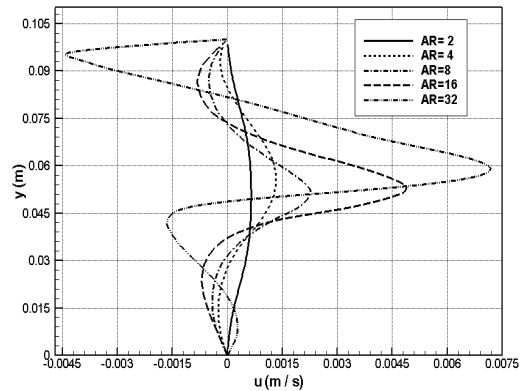


Fig. 15. Velocity distributions for different aspect ratios at $X = 6e-02$ (m), $\Phi=0\%$ and $Re=100$

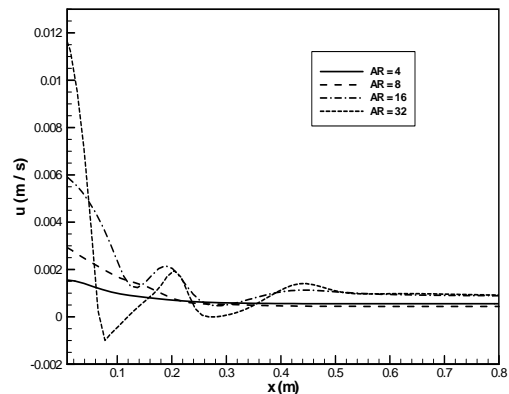


Fig. 16. Midpoint velocity at different aspect ratio at $Re=100$ and $\Phi=0\%$

REFERENCES

- [1] Chol SU. Enhancing thermal conductivity of fluids with nanoparticles. ASME-Publications-Fed. 1995 Nov 12;231:99-106.

- [2] Koblinski P, Phillpot SR, Choi SU, Eastman JA. Mechanisms of heat flow in suspensions of nano-sized particles (nanofluids). *International journal of heat and mass transfer*. 2002 Feb 28;45(4):855-63.
- [3] Li CY, Garimella SV. Prandtl-number effects and generalized correlations for confined and submerged jet impingement. *International Journal of Heat and Mass Transfer*. 2001 Sep 30;44(18):3471-80.
- [4] Battaglia F, Tavener SJ, Kulkarni AK, Merkle CL. Bifurcation of low Reynolds number flows in symmetric channels. *AIAA journal*. 1997 Jan 1;35(1):99-105.
- [5] Durst F, Melling A, Whitelaw JH. Low Reynolds number flow over a plane symmetric sudden expansion. *Journal of Fluid Mechanics*. 1974 Jun;64(1):111-28.
- [6] Rahimi-Esbo M, Ranjbar AA, Ramiar A, Arya A, Rahgoshay M. Numerical study of turbulent forced convection jet flow in a converging sinusoidal channel. *International Journal of Thermal Sciences*. 2012 Sep 30;59:176-85.
- [7] Rahimi-Esbo M, Ranjbar A.A, Ramiar A, Rahgoshay M, Arya A. Numerical study of turbulent forced convection jet flow of nanofluid in a converging duct, *International Journal Numerical Heat Transfer*. 2012 Sep 30;59:176-85.
- [8] Heris SZ, Esfahany MN, Etemad SG. Experimental investigation of convective heat transfer of Al₂O₃/water nanofluid in circular tube. *International Journal of Heat and Fluid Flow*. 2007 Apr 30;28(2):203-10.
- [9] Behzadmehr A, Saffar - Avval M, Galanis N. Prediction of turbulent forced convection of a nanofluid in a tube with uniform heat flux using a two phase approach. *International Journal of Heat and Fluid Flow*. 2007 Apr 30;28(2):211-9.
- [10] Hwang KS, Jang SP, Choi SU. Flow and convective heat transfer characteristics of water-based Al₂O₃ nanofluids in fully developed laminar flow regime. *International journal of heat and mass transfer*. 2009 Jan 15;52(1):193-9.
- [11] Al-Aswadi AA, Mohammed HA, Shuaib NH, Campo A. Laminar forced convection flow over a backward facing step using nanofluids. *International Communications in Heat and Mass Transfer*. 2010 Oct 31;37(8):950-7.
- [12] Santra AK, Sen S, Chakraborty N. Study of heat transfer due to laminar flow of copper-water nanofluid through two isothermally heated parallel plates. *International Journal of Thermal Sciences*. 2009 Feb 28;48(2):391-400.
- [13] Kalteh M, Abbassi A, Saffar-Avval M, Harting J. Eulerian-Eulerian two-phase numerical simulation of nanofluid laminar forced convection in a microchannel. *International journal of heat and fluid flow*. 2011 Feb 28;32(1):107-16.
- [14] Alinia M, Ganji DD, Gorji-Bandpy M. Numerical study of mixed convection in an inclined two sided lid driven cavity filled with nanofluid using two-phase mixture model. *International Communications in Heat and Mass Transfer*. 2011 Dec 31;38(10):1428-35.
- [15] Maninen M, Taivassalo V, Kallio S. On the mixture model for multiphase flow.
- [16] Ishii M, Hibiki T. *Thermo-fluid dynamics of two-phase flow*. Springer Science & Business Media; 2010 Nov 10.
- [17] Wen D, Ding Y. Experimental investigation into convective heat transfer of nanofluids at the entrance region under laminar flow conditions. *International journal of heat and mass transfer*. 2004 Nov 30;47(24):5181-8.
- [18] Lotfi R, Saboohi Y, Rashidi AM. Numerical study of forced convective heat transfer of nanofluids: comparison of different approaches. *International Communications in Heat and Mass Transfer*. 2010 Jan 31;37(1):74-8.
- [19] Chon CH, Kihm KD, Lee SP, Choi SU. Empirical correlation finding the role of temperature and particle size for nanofluid (Al₂O₃) thermal conductivity enhancement. *Applied Physics Letters*. 2005 Oct 10;87(15):153107.
- [20] Masoumi N, Sohrabi N, Behzadmehr A. A new model for calculating the effective viscosity of nanofluids. *Journal of Physics D: Applied Physics*. 2009 Feb 9;42(5):055501.
- [21] Lee DH, Park HJ, Ligrani P. Milliscale confined impinging slot jets: Laminar heat transfer characteristics for an isothermal flat plate. *International Journal of Heat and Mass Transfer*. 2012 Apr 30;55(9):2249-60.
- [22] Chiriac VA, Ortega A. A numerical study of the unsteady flow and heat transfer in a transitional confined slot jet impinging on an isothermal surface. *International Journal of Heat and Mass Transfer*. 2002 Mar 31;45(6):1237-48.
- [23] Lee HG, Yoon B, Ha MY. A numerical investigation on the fluid flow and heat transfer in the confined impinging slot jet in the low Reynolds number region for different channel heights. *International Journal of Heat and Mass Transfer*. 2008 Jul 15;51(15):4055-68.
- [24] Yu W, Choi SU. The role of interfacial layers in the enhanced thermal conductivity of nanofluids: a renovated Maxwell model. *Journal of Nanoparticle Research*. 2003 Apr 1;5(1-2):167-71.
- [25] Wang X, Xu X, Choi SU. Thermal conductivity of nanoparticle-fluid mixture. *Journal of thermophysics and heat transfer*. 1999 Oct 1;13(4):474-80.
- [26] Sarma A.S.R, Sundararajan T, Ramjee V. Numerical simulation of confined laminar jet flows, *International Journal of Numerical Methods in Fluids*. 2000 Jul 15;33(5):609-26.